MODELING OF THE WORKING CYCLE OF THE PRESSURE-POWERED PUMP

by

Petar I. KOLENDIĆ [a], Srbislav B. GENIĆ [a], Branislav M. JAĆIMOVIĆ [a], Nenad LJ. ĆUPRIĆ [b], Saša M. JAKIMOV [c], and Branka B. RADANOV [d]

[a] Faculty of Mechanical Engineering, University of Belgrade, Belgrade, Serbia
[b] Faculty of Forestry, University of Belgrade, Belgrade, Serbia
[c] TRACO, Belgrade, Serbia
[d] Directorate of Measures and Precious Metals, Belgrade, Serbia

Original scientific paper
DOI: 10.2298/TSCI131223021G

This paper presents an analysis of working parameters of the pressure-powered pump. Mathematical models for determining the pump filling and discharge periods were developed and statistically compared to experimental results. The statistical parameters of the final correlation between here presented mathematical model and experimental results are in the acceptable range. Pump characteristics are presented in the common manner: in the form of the pump head vs. capacity diagram.

Key words: *pressure-powered pump, pump working cycle, filling period, discharge period, condensate recovery*

Introduction

A device designed to move liquids using the energy of pressurized air, inert gas or steam is called a "Pressure-Powered Pump" (PPP), "pressure motive pump" or "motor-less pump" [1]. This device enables flow of the liquid (primary fluid) by using the secondary fluid (steam, pressurized air or inert gas), which fills the pump volume periodically. In other words, the secondary fluid functions like a piston or a membrane, which pump the primary fluid.

The working cycle of the PPP has two phases (fig. 1): the filling or intake period and discharge or exhaust period. During the filling period liquid (primary fluid) enters the pump vessel through an inlet check valve. The float moves upward, while the exhaust valve is opened. After having achieved high liquid level(HLL) the float-actuated device opens the secondary fluid valve and closes the exhaust valve. The secondary fluid enters the pump volume; the pressure within the vessel rises and enables the liquid from the vessel to flow through the outlet check valve. When the liquid level drops to low liquid level (LLL) the float closes the secondary fluid valve and opens the exhaust valve, so the next cycle can start. The mechanism of PPP enables reliable operation under variable operating conditions as non-electric, seal-less, and maintenance-free pumping device [2, 3].

* Corresponding author; e-mail: pkolendic@mas.bg.ac.rs

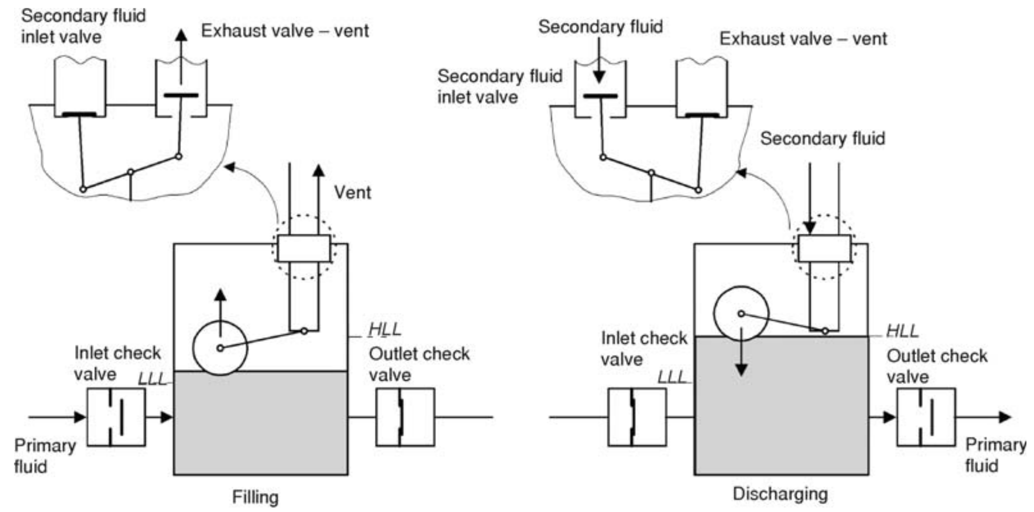

Figure 1. The working cycle of a PPP (arrows denote the flow of fluids and direction of the moving of the float)

When the liquid pressure in the suction side of the pump is low or near by the saturation pressure, the centrifugal pumps can be exposed to cavitation. These scenarios include the following: transport or drainage of condensate in the pipelines, pressure or vacuum vessels, manholes, pits, swimming pools, wells, *etc*. For these cases, it is useful to consider using of PPP instead of centrifugal pumps, as the cavitation problems can be avoided.

According to the Directive 2010/31/EU of the European Parliament and of the Council of May 19, 2010, on the energy performance of buildings, the new buildings occupied and owned by public authorities have to be nearly zero-energy buildings after the end of 2018, and after the end of 2020 all new buildings will be nearly zero-energy buildings (Article 9) [4].

The growth of energy consumption of HVAC systems is particularly significant: 50% of building consumption and 20% of total consumption in the USA [5]. The modern PPP with a precisely balanced working cycle can be used as energy saving devices [6]. This is especially prominent for the condensate return lines since the PPP does not need electrical energy to pump the condensate. Instead, the steam that is already available in the facility is used to pump the condensate back to the boiler [1, 7-10]. Implementation of a condensate recovery system is a primary energy saving attempt. With this investment an owner can obtain 10 to 20% of potential energy savings in a building [11, 12]. As condensate has two to four times higher temperature than that of the makeup water, the energy savings can be realized by returning condensate to the boiler. This is recommended in cases when condensate is not contaminated in the process. Also, the lost of "blowdown water" in the steam boilers will be lower. Therefore, the following energy savings can be considered due to [7]:
– less consumption of the boiler fuel as less energy is need to convert the condensate to steam,
– less consumption of water treatment chemicals, and
– lower costs of boiler feed-water supply.

The condensate recovery systems find their implementation in HVAC systems, as additional sources of water for the cooling towers. For instance, the condensate from the cooling coils could be collected and pumped back into the cooling tower make-up water pipeline [13, 14].

The PPP can also be used for pressure maintenance in heating system installations (expansion tanks) and for the pressure rise in the water supply systems. Using of PPP can be also beneficial in hazardous areas, or in cases of transport of aggressive and/or flammable liquids [15].

As pump manufacturers usually provide a set of capacity curves for their pumps when handling water at different temperatures [7, 16], the designers, field and plant engineers have to rely on available tabulated data or diagrams. On the other hand there are practically none transient data regarding PPP cycles [17]. The aim of this paper is to validate the established mathematical model of a PPP cycle by using unique experimental results and to explain the main working features.

The experimental set-up and measuring method

There are many companies worldwide that manufacture PPP; some of them are widely known and some operate only on a small scale (national markets). For our experimental investigation we used the PPP "Elephant" manufactured by the Serbian company "Traco" from Belgrade [18].

This study was conducted in order to correlate the duration of the working cycle with the working conditions such as the pressure of the secondary fluid and pump head. The experimental set-up is schematically presented on fig. 2. The primary fluid was water and the secondary fluid was compressed air from a compressor (1). Water was introduced into the pump vessel (2) by gravity from a tank (3). After the filling period the water from the vessel was pushed, by compressed air, back to the tank (3). Valve (4) was used for water flow rate regulation. The diameters of the inlet pipeline were: DN25, DN40, DN50, and DN80. The diameter of the outlet pipeline was DN 50. The compressor was connected to the pump vessel by a 9 mm diameter hose.

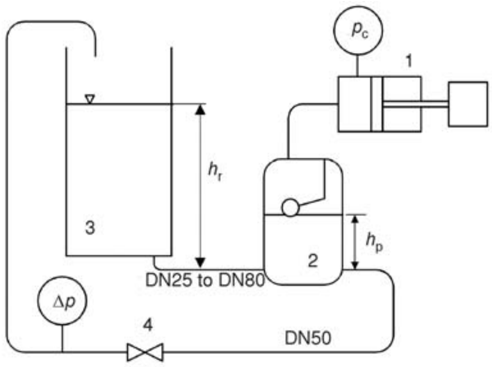

Figure 2. Experimental set-up

The following values were measured during the experiments:
h_r [m] is the water level in tank, h_p [m] – the water level inside the pump, p_c [bar] – the gauge pressure of compressed air, τ_f [s] – the duration of filling period, τ_d [s] – the duration of discharge period, and Δp [bar] – the the pump head (outlet pipe resistance).

Ninety eight experimental runs were conducted and working parameters during the experimental work were as follows:
- the pressure of compressed air was 2-6 bar,
- the pump head was up to 6 bar,
- the maximal flow rate (pump capacity) was up to $V = 9$ m^3/h,
- the height of the water level in the tank was h_r = 880-3000 mm, and
- the absolute pressure in the pump vessel was between atmospheric pressure (1 bar) and 2.5 bar.

Duration of characteristic PPP periods was measured by chronometer watch, pressures were measured using manometer with Bourdon tube (class 0,6), and the heights of the water level were measured by simple metre with millimeter scale.

Modeling of the PPP cycle

As explained before, the working cycle of the PPP "Elephant" consists of the filling period and discharge period, so parameters for these two phases have been analyzed separately.

Modeling of the pump filling period

Mathematical modeling of the pump filling period

The process of filling of the pump vessel is presented on fig. 3.

Based on the equation of continuity it follows:

$$w_\mathrm{r} A_\mathrm{r} = w_\mathrm{f} A_\mathrm{f} = w_\mathrm{p} A_\mathrm{p} \tag{1}$$

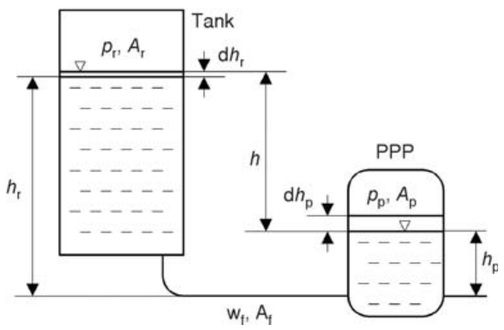

Figure 3. Schematic representation of the pump filling process

where w_r [ms^{-1}] is the discharge velocity of the tank, A_r [m^2] – the area of the cross-section of the tank, w_p [ms^{-1}] – the velocity of water in the pump vessel, A_p [m^2] – the cross-sectional area of the pump vessel, w_f [ms^{-1}] – the water velocity in the inlet pipe, and A_f [m^2] – the cross-sectional area of the inlet pipe:

$$A_\mathrm{f} = \frac{\pi d_\mathrm{f}^2}{4} \tag{2}$$

and d_f [m] is the inlet pipe inside diameter.

Based on Bernoulli's equation it follows:

$$\frac{\rho w_r^2}{2} + p_r + \rho g h = \frac{\rho w_r^2}{2} + p_p + \Delta p_\mathrm{loss} \tag{3}$$

and the mass balance equation is:

$$w_\mathrm{f} A_\mathrm{f} \mathrm{d}\tau_\mathrm{f} = -A_\mathrm{r} \mathrm{d}h_\mathrm{r} = A_\mathrm{p} \mathrm{d}h_p \tag{4}$$

where ρ [kgm^{-3}] is the density of water, p_r [Pa] – the absolute pressure in the tank (atmospheric pressure), g = 9.81 m/s^2 is the gravitational acceleration, h [m] – the difference between the water levels in the tank and in the pump, p_p [Pa] – the absolute pressure in the pump vessel, Δp_loss [Pa] – the pressure drop in the inlet pipeline, and h_p [m] – the water level in the pump vessel.

The pressure drop in the inlet pipeline is:

$$\Delta p_\mathrm{loss} = \left(f_\mathrm{f} \frac{L_\mathrm{f}}{d_\mathrm{f}} + K_\mathrm{f} \right) \frac{\rho w_f^2}{2} = C_\mathrm{f} \frac{\rho w_f^2}{2} \tag{5}$$

where C_f is the coefficient of the overall flow resistance, f_f – the friction factor, K_f – the local resistance coefficient, and L_f [m] – the length of inlet pipe.

The water velocity through the inlet pipeline is:

$$w_\mathrm{f} = \sqrt{\frac{2gh + \dfrac{2}{\rho}(p_\mathrm{r} - p_\mathrm{p})}{C_\mathrm{f} + \left(\dfrac{A_\mathrm{f}}{A_\mathrm{p}}\right)^2 - \left(\dfrac{A_\mathrm{f}}{A_\mathrm{r}}\right)^2}} \tag{6}$$

The change of the fluid level height in the tank and the pump is:

$$-\mathrm{d}h = -\mathrm{d}h_\mathrm{r} + \mathrm{d}h_\mathrm{p} \tag{7}$$

from where follows:

$$w_\mathrm{f}\mathrm{d}\tau_\mathrm{f} = -\frac{\dfrac{A_\mathrm{p}}{A_\mathrm{f}}}{1+\dfrac{A_\mathrm{p}}{A_\mathrm{r}}}\mathrm{d}h \tag{8}$$

so the differential equation for filling time is:

$$\mathrm{d}\tau_\mathrm{f} = -\frac{\dfrac{A_\mathrm{p}}{A_\mathrm{f}}}{1+\dfrac{A_\mathrm{p}}{A_\mathrm{r}}}\sqrt{\frac{\mathrm{C}_\mathrm{f} + \left(\dfrac{A_\mathrm{f}}{A_\mathrm{p}}\right)^2 - \left(\dfrac{A_\mathrm{f}}{A_\mathrm{r}}\right)^2}{2gh + \dfrac{2}{\rho}(p_r - p_p)}}\mathrm{d}h \tag{9}$$

The difference between water levels in the tank and in the pump is *LLL* [m] at the start of the filling period [$\tau = 0$], and *HLL* [m] at the end of the filling period [$\tau = \tau_\mathrm{f}$], so after solving the eq. (9) the duration of the filling period is:

$$\tau_\mathrm{f} = \sqrt{\frac{2}{g}}\frac{\sqrt{1 + C_\mathrm{f} + \left(\dfrac{A_\mathrm{p}}{A_\mathrm{f}}\right)^2 - \left(\dfrac{A_\mathrm{p}}{A_\mathrm{r}}\right)^2}}{1+\dfrac{A_\mathrm{p}}{A_\mathrm{r}}}\left(\sqrt{LLL + \frac{p_\mathrm{r} - p_\mathrm{p}}{\rho g}} - \sqrt{HLL + \frac{p_\mathrm{r} - p_\mathrm{p}}{\rho g}}\right) \tag{10}$$

Analysis of experimental results for the pump filling period

The experimental results obtained during the pump filling period were analyzed using the least squares method, taking into consideration the derived theoretical eq. (10). Monitoring of pump behavior showed that the suction duration depends on the compressed air pressure, so this parameter was included into the correlation:

$$\tau_f^C = C\left(\sqrt{h_\mathrm{r} + \frac{p_\mathrm{r} - p_\mathrm{p}}{\rho g}} - \sqrt{h_\mathrm{r} - 0.3\frac{p_\mathrm{r} - p_\mathrm{p}}{\rho g}}\right)p_c^{0.2} \tag{11}$$

where τ_f^C [s] is the correlated duration of the filling period and p_c [bar] is the gauge pressure of the compressed air. Water level height in the tank h_r was measured from the axis of the inlet pipeline. According to measurements, the parameter *C* depends on the diameter of the inlet pipeline and on the type of the check valve. The experimentally determined values for the constant *C* and the root-mean square deviation (RMSD) are given in tab. 1, and correlation field is presented in fig. 4.

Table 1. Values of parameter *C* and the RMSD for eq. (11)

DN	C	RMSD, [%]
25	252	10.69
40	133	11.92
50	49	12.30
80	40	7.88

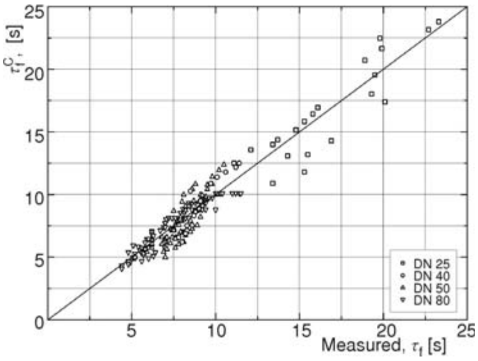

Figure 4. Measured *vs.* experimental filling time data during the filling period of the pump

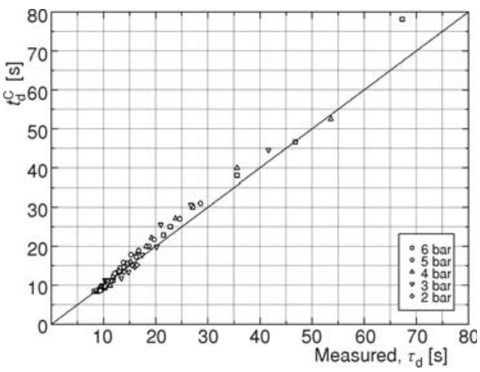

Figure 5. Measured *vs.* calculated discharged period data during the pump discharge period

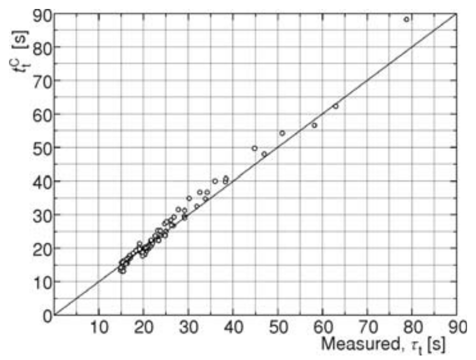

Figure 6. Correlation field for the complete PPP working cycle

Modeling of the pump discharge process

Statistical modeling of the pump intake volume

In each working cycle the pump was filled up to a specified volume. It was noticed that this filling volume mostly depends on the air pressure. Based on the statistical analysis of the experimental results, the following equation was obtained:

$$V_p^C(p_c) = 0.0248 + 0.00152 p_c \tag{12}$$

where V_p^C [m^3] is the correlated filling volume. The RMSD of the pump intake volume is 0.89%.

Statistical modeling of the pump discharge period

Based on the statistical analysis of the experimental results, the following equation for the discharge duration period was obtained:

$$\tau_d^C = \frac{43 - 7p_c + 0.67p_c^2}{\ln\left(\dfrac{p_c}{\Delta p}\right)} \tag{13}$$

where τ_d^C [s] is the correlated discharge period and Δp [bar] is the pump head. The correlation field for the discharge duration period is shown in fig. 5. The RMSD of the pump intake volume is 7.80%.

Analysis of the complete working cycle of PPP

The working cycle consists of the filling and discharging period. The total duration of a working cycle is:

$$\tau_t = \tau_f + \tau_d \tag{14}$$

and the correlated time of the working cycle is calculated using eqs. (11) and (13)

$$\tau_t^C = \tau_f^C + \tau_d^C \tag{15}$$

The correlation field for the total duration of the working cycle is presented in fig. 6. The RMSD of the correlated and measured values is 5.82 %.The diagram in fig. 7 shows all measured working cycles in the form of a pump head *vs*. capacity diagram. Pump capacity V [m^{3}h^{-1}] is the discharge flow rate reduced to the complete PPP working cycle.

Conclusions

Th PPP working cycle consists of two periods: the filling (or intake) and discharge (or exhaust) period. In the present paper, an analysis of both working periods of PPP was analyzed through experimental work and mathematical modeling. Correlations for each period were established in order to connect the process variables of PPP.

Experiments and mathematical modeling presented in the paper, as well as the statistical analysis of correlations, was the basis for establishing the diagram of PPP head vs. capacity. Since the statistical parameters are in the narrow and acceptable range, presented modeling adequately describes the working cycle of the PPP and it can be used further on for research of other types of PPP.

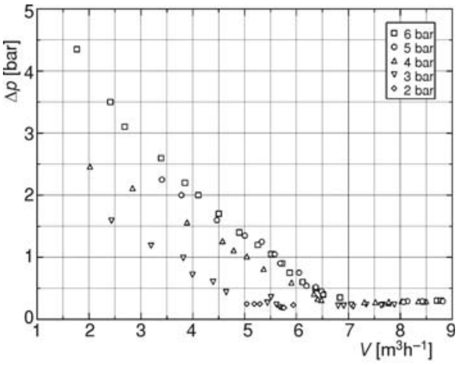

Figure 7. PPP head *vs.* capacity diagram – measured values

Generally speaking there are three cases that govern the PPP selection for the engineering application:

– the pump capacity (V, [m^{3}h^{-1}]) is determined on the basis of the required pump head and secondary fluid pressure,
– the pump head (Δp, [bar]) is determined on the basis of the required pump capacity and secondary fluid pressure, and
– on the basis of pump head and pump capacity engineer should determine the pressure of the secondary fluid (p_c, [bar]).

Manufacturers and suppliers of th PPP provide diagrams or tabulated data that are used by designers, plant or field engineers. These diagrams are generated from the experimental results, which are post-processed as presented in this paper. The example of the final diagram form is presented in fig. 8.

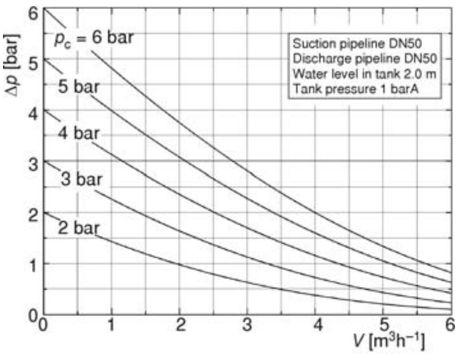

Figure 8. PPP head *vs.* pump capacity diagram from a manufacturer's catalog [18]

The main benefit of modeling presented in this paper is the following.

- It provides the description of experimental set-up for PPP cycle analysis.
- The simplified research basis (mathematical modeling) is suitable for any engineer that has to analyze the working cycle of any PPP pump.

Acknowledgement

We thank the Ministry of Education, Science and Technological Development of Serbia for partial support of this study through the Project of Energy Efficiency.

Nomenclature

A_r – cross-sectional area of the tank, [m^2]
A_p – cross-sectional area of the pump vessel, [m^2]
A_f – cross-sectional area of the inlet pipe, [m^2]
C – parameter
C_f – overall flow resistance coefficient

d_f – suction (inlet) pipe inside diameter, [m]
f_f – friction factor
g – gravitational acceleration, [ms^{-2}]
HLL – high liquid level height, [m]
h – difference between the water levels in the tank and in the pump, [m]
h_r – water level in the tank (measured from the axis of the inlet pipeline), [m]
h_p – water level in the pump vessel, [m]
K_f – local resistance coefficient
LLL – low liquid level height, [m]
L_f – length of inlet pipe , [m]
p_c – gauge pressure of the compressed air, [bar]
p_p – absolute pressure in the pump vessel, [Pa]
p_r – absolute pressure in the tank, [Pa]
Δp – the pump head (outlet pipe resistance)
Δp_{loss} – pressure drop in the inlet pipeline, [Pa]
RMSD – root-mean square deviation
V – pump capacity, [m^{3}h^{-1}]
V_p – filling volume, [m^3]
w_f – water velocity in the inlet pipe, [ms^{-1}]
w_p – water velocity in the pump vessel, [ms^{-1}]
w_r – discharge velocity of the tank, [ms^{-1}]

Greek symbols

ρ – density of water, [kgm^{-3}]
τ – time, [s]
τ_d – duration of discharge period, [s]
τ_f – duration of filling period, [s]
τ_t – total duration of a working cycle, [s]

Superscript

C – correlated

References

[1] Langley, C., Sacks, A., *Steam and Hot Water Primer*, Delmar, CENGAGE Learning, 2010, ISBN-10: 1-4283-6072-7
[2] ***, Pressure Operated Condensate Return Pumps, A Division of Richards Industries, 2013 http://www.ovisinc.com/documents/PressureOperatedCondensateReturnPumps.pdf.
[3] ***, Chicago Industrial Pump Company, 2013 http://www.pitbullpumps.com/resources/uploads/pdfs/NewslettercondensateCV.pdf
[4] ***, Directive 2010/31/EU of the European Parliament and of the Council of 19 May 2010 on the Energy Performance of Buildings
[5] Perez-Lombard, L., *et al*., A Review on Buildings Energy Consumption Information, *Energy and Buildings, 40* (2008), 3, pp. 394-398
[6] ***, Condensate Pump Reduces Energy Consumption, *World Pumps, 482* (2006), Nov. p. 9
[7] ***, http://www.spiraxsarco.com/
[8] Brader, J. S., Rocheleau, D. N., Failure Analysis and Redesign of a Pressure Powered Pump Mechanism, *Proceedings*, ASME International Mechanical Engineering Congress and Exposition, New York, USA, 2001, pp. 1-6
[9] ***, High Temperatures and Danger of Impeller Cavitation is the Major Challenge of Condensate Pumping, 2013, http://www.engineeringtoolbox.com/condensate-pumping-d_280.html
[10] ***, *Operation and Maintenance: Small Heating Systems*, Department of the Army Technical Manual, Headquarters Department of the Army, USA, 1990
[11] Draganici, G., *et al*., Green House – a Concept Less Known – Integrated Design Method, *Proceedings*, 3rd International Conference on Environmental and Geological Science and Engineering, Constantza, Romania, 2010, 137-142, ISBN: 978-960-474-221-9
[12] ***, *Energy Efficiency in Buildings*, CIBSE Guide F, 2nd ed., The Chartered Institution of Building Services Engineers, London, 2004, ISBN 1 903287 34 0
[13] Morder, M., INOVA South Patient Tower, Mechanical Option – Final Report, 2012 http://www.engr.psu.edu/ae/thesis/portfolios/2012/mtm5093
[14] Johnson, G. R., HVAC Design for Sustainable, *ASHRAE Journal, 50* (2008), Sept., pp. 24-34
[15] Nesbitt, B., *Handbook of Pumps and Pumping*, Elsevier Science & Technology Books, 2006, ISBN: 185617476X.
[16] Mobley, R. K., P*lant Engineer's Handbook*, Elsevier Butterworth-Heinemann, 2001, ISBN: 0750673281
[17] Oughton, D., Hodkinson, S., *Faber & Kell's Heating & Air-Conditioning of Buildings*, Rutledge, 2008, ISBN: 0750683651
[18] ***, http://www.traco.rs/

Paper submitted: December 22, 2013
Paper revised: February 18, 2015
Paper accepted: February 18, 2015